International Journal of Medical, Medicine and Health Sciences
ISSN: 2517-9969
Vol:11, No:9, 2017

Investigation of Wave Atom Sub-Bands via Breast Cancer Classification

Nebi Gedik, Ayten Atasoy

***Abstract*—**This paper investigates successful sub-bands of wave atom transform via classification of mammograms, when the coefficients of sub-bands are used as features. A computer-aided diagnosis system is constructed by using wave atom transform, support vector machine and k-nearest neighbor classifiers. Two-class classification is studied in detail using two data sets, separately. The successful sub-bands are determined according to the accuracy rates, coefficient numbers, and sensitivity rates.

***Keywords*—**Breast cancer, wave atom transform, SVM, k-NN.

I. Introduction

BREAST cancer, a type of cancer which is a frequent cause of death, commonly occurs among women. Thus, its detection in early phases is crucial to fight the disease [1]. Another important thing about breast cancer is the classification of breast cancer as benign or malignant [2], [3]. Mammograms are the best available tools to accomplish these important goals. However, the process of diagnosis is a very difficult task. So, 10–30% of cancer cases are missed by radiologists [4]. Furthermore, non-cancerous lesions are misinterpreted. To avoid the risks mentioned above, computer-aided diagnosis (CAD) systems as a second opinion provider are aimed to aid the radiologists to reduce false positive and false negative rates [5]-[9].

In the present study, a mammogram classification system is constructed to investigate wave atom transform. The scope of the system is to analyze wave atom transform to take advantage of its property that is capturing both the coherence of the pattern along the oscillations and the pattern across the oscillations. Because of this property, wave atom transform generates coefficients that can be naturally arranged as two matrices (coefficients' packets) for every scale. In order to explore the different aspects of this algorithm, the aim is to determine which packet will provide the maximum classification accuracy. The classification is performed in two successive stages: distinguishing between normal and abnormal regions, and classifying tumors as malignant or benign. To do so two different classifiers are employed (SVM, and k-NN). In summary; the investigation in this paper are explored in three: determination of the most successful packet and scale of the wave atom sub-bands, comparing the results using two different classifiers and test the results using two different databases.

The remainder of the paper is organized as follows: Sections II and III include related works and a brief introduction of wave atom transform respectively. Materials and methods are described in Section IV, and the results and discussion are presented in Section V. Sections VI and VII contain the experiment and the conclusions.

II. Related Works

The diagnostic performance of CAD systems, particularly, depends on the feature extraction step which performs a key function. If the feature set has a high representational power, compactness and good discrimination ability, speed and classification accuracy of the CAD systems are greatly improved [10]. Therefore, in the literature, many studies have focused on this issue. Among the proposed feature extraction methods, multi-resolution analysis techniques such as contourlet, wavelet and curvelet transform draw attention. Liu et al. [11] propose a system that includes multi-resolution analysis to detect speculated lesions in digital mammograms. The system uses a linear phase non-separable two-dimensional wavelet transform to represent the mammograms. The feature set is composed using the coefficients of the wavelet pyramid at each resolution. A binary tree classifier is used to detect abnormalities. The results show that the system is capable of detecting abnormalities in different sizes at low false positive rates. Ferreira et al. [12] construct a system to extract and select the best features from the images to solve the difficulties of classifying them as benign, malignant or normal ones. The feature extraction process is performed using special sets of the coefficients after transforming the images in a wavelet basis. The results of the system are very promising. Ergin et al. [13] use a combination consisting of the histogram of oriented gradients (HOG), dense scale-invariant feature transform (DSIFT) and local configuration pattern (LCP) methods to classify breast cancer cases. These methods are able to extract the rotation- and scale-invariant features for all tissue types. The classification is made using support vector machine (SVM), k-nearest neighbor (k-NN), decision tree, and Fisher linear discriminant analysis (FLDA).

Moayedi et al. [14] use the contourlet transform which is a powerful and developed version of Discrete Wavelet Transform. From the system, initially, regions of interest are obtained using a preprocessing step to remove the pectoral muscles. The feature extraction is performed utilizing the contourlet transform, and then feature set is created using the contourlet coefficients. A genetic algorithm is employed as feature selection to get most distinctive features. The

Nebi Gedik is with the Faculty of Marine Sciences at Karadeniz Technical University Trabzon, Turkey (phone: +90 462 377 8066, corresponding author, e-mail: ngedik@ktu.edu.tr).

Ayten Atasoy is with the Faculty of Engineering at Karadeniz Technical University Trabzon, Turkey (e-mail: ayten@ktu.edu.tr)

classification is carried out using the feature set based on successive enhancement learning (SEL) weighted SVM, support vector-based fuzzy neural network (SVFNN) and kernel SVM. Jasmine et al. [15] represent a system combining non-subsampled contourlet transform (NSCT) and SVM to classify masses in digitized mammograms. The aim of mass classification is to extract the features from the contourlet coefficients by applying to the image and feeding the SVM classifier with the outcomes. Pak et al. [16] propose an algorithm for breast cancer detection and classification using NSCT. In their paper, the regions of interest (ROIs) are enhanced using NSCT, then, the super-resolution (SR) algorithm is used to increase the resolution of them, and a high-pass filter is also utilized to highlight the desired regions. Seven features based on regional, boundary and density descriptors are extracted to classify images as normal and abnormal. For malign or benign separation, each feature is analyzed by calculating skewness of itself. The classification is carried out using the AdaBoost algorithm. Eltoukhy et al. [17] investigate the curvelet transform comparing it with the wavelet transform on digital mammogram images. In that paper, a Euclidean distance classifier is employed to distinguish mammograms using a multi-scale curvelet transform coefficients. A set of the biggest coefficients extracted from each scale level of the curvelet transform is used as the feature vector. The result is 98.59% when normal-abnormal classification is performed. Francis et al. [18] propose an algorithm using the curvelet transform for abnormality detection in breast thermograms. Thermograms are transformed the curvelet domain, then statistical and texture features are obtained from curvelet coefficients. The resulted set is used to feed the SVM classifier. Abnormal thermograms are detected with an accuracy of 90.91%.

Recently, wave atom transform is presented as a multi-scale and multi-directional transform. The transform has been used in different areas with different goals [19]-[21]. Rajesh et al. [22] designed a CAD system to classify micro-calcification in mammograms. The feature vectors are created by the system calculating energy values of wave atom coefficients. SVM is used as a classifier. Elangeeran et al. [23] also proposed a system to classify cases of micro-calcifications using wave atom. Circular complex-valued extreme learning machine (CC-ELM) is employed to characterize the micro-calcifications as benign or malignant. The features obtained from wave atom coefficients are reduced using principal component analysis (PCA). Gedik et al. [24] developed a CAD system that uses the wave atom transform including all abnormalities in mammograms. The system uses the features that are generated from wave atom coefficients. The SVM classifier is used to classify mammograms and PCA is employed to increase the classification success rate. The best success rates are obtained at scales 1, 2, and 3 with the combination of SVM and PCA.

III. Wave Atom Transform

The wave atom transform introduced by Demanet and Ying in [25] is a member of the family of oriented multi-scale transforms. The transform is a variant of 2-D wavelet packets obeying parabolic scaling relation, i.e.: the wavelength is taken proportional to the square of the diameter. Besides having better frequency localization, which is a problem for filter banks, wave atoms produce an expansion of oscillatory functions or oriented textures which are significantly sparser than any other multi-resolution representations.

Two parameters, α and β are used to characterize the wave atom transform among the other existing transforms. These parameters can be used to classify most of the known architectures of wave packets. Using this description, the connections between various transforms have been clarified. α indicates whether the decomposition is multi-scale (α = 1) or not (α = 0). On the contrary, β indicates whether basis elements are localized and poorly directional (β = 1) or extended and fully directional (β = 0). Fig. 1 illustrates the classification of multi-resolution transforms according to α and β.

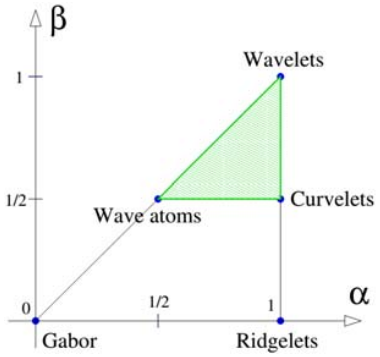

Fig. 1 Illustration of the architectures of different wave packets according to (α, β) [25]

Wave atoms are the elements of a frame of wave packets $\{\varphi_\mu\}$, indexed by an integer parameter M for all $M > 0$,

$$|\hat{\varphi}_\mu(\omega)| \le C_M \cdot 2^{-j}(1 + 2^{-j}|\omega - \omega_\mu|)^{-M} + C_M \cdot 2^{-j}(1 + 2^{-j}|\omega + \omega_\mu|)^{-M} \quad (1)$$

$$|\varphi_\mu(x)| \le C_M \cdot 2^j(1 + 2^j|x - x_\mu|)^{-M}, \quad (2)$$

As a formal definition of 2-D wave atom, $\varphi_\mu(x)$ is a function indexed by a multiple subscript $\mu = (j, m, n) = (j, m_1, m_2, n_1, n_2)$ which in turn (x_μ, ω_μ) in phase space which is $x_\mu = 2^{-j}n$, $\omega_\mu = \pi 2^j m$, $C_1 2^j \le \max_{i=1,2}|m_i| \le C_2 2^j$ where $C_1, C_2 > 0$. Therefore, x_μ is the position vector and it is the center of $\varphi_\mu(x)$ whereas the wave vector ω_μ determines the centers in the frequency space of both bumps of $\hat{\varphi}_\mu(\omega)$ (centered at $+\omega_\mu$ and $-\omega_\mu$) [25]. These representations belong to a qualitative description of wave atom with spatial frequency location restriction. In practice, Demanet [25] constructs wave atom via tensor products of adequately chosen 1D wave packets using the strategy of frequency localization.

Firstly, a 1D family of real-valued wave packets $\psi_{m,n}^j(x)$

are constructed in frequency, providing $j \geq 0$, $m \geq 0$, $n \in Z$, around $\pm\omega_{j,m} = \pm\pi 2^j m$, with $C_1\, 2^j \leq m \leq C_2\, 2^j$.

$$\psi_{m,n}^{j}(x) = \psi_{m}^{j}(x - 2^{-j}n) = 2^{j/2}\psi_{m}^{0}(2^j x - n) \tag{3}$$

$$\psi_{m}^{0}(\omega) = e^{-i\omega/2}\left[e^{i\alpha_m} g\left((-1)^{\mathrm{m}}\left(\omega - \pi\left(m + \tfrac{1}{2}\right)\right)\right) + e^{-i\alpha_m} g\left((-1)^{\mathrm{m}+1}\left(\omega + \pi\left(m + \tfrac{1}{2}\right)\right)\right)\right] \tag{4}$$

where $\alpha_{\mathrm{m}} = \frac{\pi}{2}(\mathrm{m} + \frac{1}{2})$, and g is a C^{∞} bump function. Calling H the Hilbert transform, $H\psi_{m,n}^{j}$ is another orthonormal basis. In the frequency domain, Hilbert transformation expresses as:

$$\widehat{H\psi_{m,n}^{j}}(\omega) = -i\hat{\psi}_{m,n,+}^{j}(\omega) + i\hat{\psi}_{m,n,-}^{j}(\omega) \tag{5}$$

where $(-,+)$are the positive and negative frequencies whose components have $(-i, i)$ as their respective weights. Providing $\mu = (j, m, n) = (j, m_1, m_2, n_1, n_2)$, two orthonormal basis are defined dually as:

$$\varphi_{\mu}^{+}(\mathrm{x}_1, \mathrm{x}_2) = \psi_{\mathrm{m}_1}^{\mathrm{j}}(\mathrm{x}_1 - 2^{-\mathrm{j}}\,\mathrm{n}_1)\,\psi_{\mathrm{m}_2}^{\mathrm{j}}(\mathrm{x}_2 - 2^{-\mathrm{j}}\,\mathrm{n}_2) \tag{6}$$

$$\varphi_{\mu}^{-}(\mathrm{x}_1, \mathrm{x}_2) = \mathrm{H}\psi_{\mathrm{m}_1}^{\mathrm{j}}(\mathrm{x}_1 - 2^{-\mathrm{j}}\,\mathrm{n}_1)\,\mathrm{H}\psi_{\mathrm{m}_2}^{\mathrm{j}}(\mathrm{x}_2 - 2^{-\mathrm{j}}\,\mathrm{n}_2) \tag{7}$$

The tight frame (8) for wave atom is formed by using (3) and (4):

$$\varphi_{\mu}^{(1)} = \frac{\varphi_{\mu}^{+} + \varphi_{\mu}^{-}}{2}, \qquad \varphi_{\mu}^{(2)} = \frac{\varphi_{\mu}^{+} - \varphi_{\mu}^{-}}{2} \tag{8}$$

IV. Materials and Methods

Two data sets are used to investigate the wave atom sub-bands, obtained from The Mammographic Image Analysis Society (MIAS) and The Digital Database for Screening Mammography (DDSM). Both databases have been classified by technically experienced radiologists, and their contents and the radiologists' classifications are publicly available [26], [27].

Two sets of ROI are composed of 228 images that were obtained from these databases separately. ROIs are obtained by manual cropping operation in size of 128x128 pixels from the original mammograms. In cropping operation, the centers of the ROIs correspond to the centers of abnormality determined by expert radiologists. Selection of ROIs in normal mammograms is randomly made, including all tissue types (fatty, fatty glandular, dense glandular) with approximately same probability. The distribution of the ROI images used in this study is illustrated in Table I for both MIAS and DDSM. Both ROI sets include the same number of images with regard to abnormality and tissue type. The ROI set obtained from MIAS database includes all abnormalities in the database (except one that was not appropriate for cropping). The ROI set obtained from the DDSM database is constructed in the same way as for the MIAS ROI set.

TABLE I
Distribution of ROIs

Class	Benign	Malignant	Total
Abnormal	64	50	114
Normal	–	–	114
Total			228

Every ROI set is used by dividing into two sets: a training set, which is constructed with 70% of the ROIs, and a testing set made with the remaining 30%. The classification process is evaluated using two classifiers; SVM and k-NN. SVM optimization is performed using 10-fold cross-validation. k-NN is applied for 31 different k values, from 3 to 63. The classification is carried out to solve two mammogram classification problems: The classification of normal versus abnormal cases and that of benign versus malignant.

Once two separate ROI sets are constructed and divided into training and testing parts, wave atom transform is applied to ROI sets. Finally, the coefficients of the transform are obtained as features. The coefficients are grouped in two packets (we call these as the first and second packet) for each scale, and the transform is applied at four scales. Hence, eight different feature vectors are constructed using the coefficients of each packet. These feature vectors are used to feed the classifiers. The system can be summarized as shown in Fig. 2.

V. Experiment

This section presents the classification task in two stages, normal-abnormal and benign-malignant classification. In the first place, the classification of normal versus abnormal cases is performed, and wave atom is applied to the dataset for feature extraction as in the illustration of Fig. 2. Then, the feature vectors are individually built using the coefficients of each packet, and those are used to feed SVM and k-NN classifiers.

Table II illustrates the performance of the classifications to distinguish mammograms as either normal or abnormal using the ROIs obtained from the MIAS database. When the first packets of the scales are used, the best classification performances are 98.53% for the SVM classifier with scale 1 and 82.35% for the k-NN classifier with scale 1. In terms of the second packets of the scales, the best classification performances are 100% for the SVM classifier with scale 1 and 77.94% for the k-NN classifier with scale 1.

The second stage of the classification is to distinguish mammograms as benign or malignant. Table III illustrates the performance of the SVM and k-NN classifiers during the benign-malignant separation by using the ROIs obtained from the MIAS database. The maximum accuracy rates obtained by using the first packets of the scales are 91.18% for SVM classifier with scale 2 and 88.24% for the k-NN classifier with scale 1. The results, according to the second packets, are 91.18% for the SVM classifier with scale 1 and 88.24% for the k-NN classifier with scale 2.

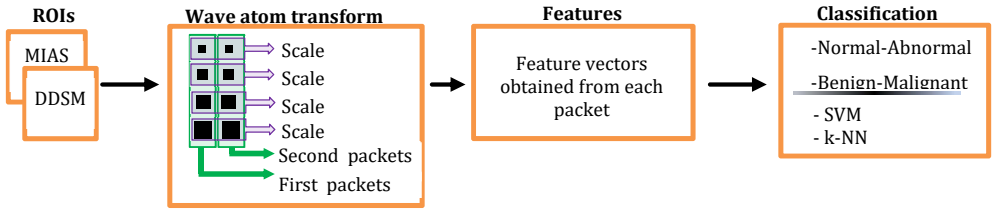

Fig. 2 Illustration of the structure of the system in this paper

TABLE II
THE CLASSIFICATION RESULTS OF NORMAL-ABNORMAL CASES BY USING THE ROIS OBTAINED FROM MIAS DATABASE

Packets	Scale (number of coefficients)	SVM			k-NN			
		Accuracy (%)	Specificity	Sensitivity	Accuracy (%)	Specificity	Sensitivity	k value
First	1 (16)	98.53	1	0,97	82.35	1	0.65	3
	2 (560)	75	1	0.5	45.59	0.74	0.18	3
	3 (5824)	60.29	1	0.21	45.59	0.71	0.21	3
	4 (9984)	58.82	1	0.18	47.06	0.71	0.24	3
Second	1 (16)	100	1	1	77.94	0.56	1	27
	2 (560)	75	1	0.5	42.65	0.68	0.18	3
	3 (5824)	60.29	1	0.21	42.65	0.68	0.18	3
	4 (9984)	58.82	1	0.18	47.06	0.71	0.24	3

TABLE III
THE CLASSIFICATION RESULTS OF BENIGN-MALIGNANT CASES BY USING THE ROIS OBTAINED FROM MIAS DATABASE

Packet	Scale (number of coefficients)	SVM			k-NN			
		Accuracy (%)	Specificity	Sensitivity	Accuracy (%)	Specificity	Sensitivity	k value
First	1 (16)	64.71	0.53	0.74	88.24	1	0.79	19
	2 (560)	91.18	0.8	1	85.29	0.73	0.95	11
	3 (5824)	70.59	0.33	1	82.35	1	0.69	7
	4 (9984)	64.71	0.2	1	85.29	0.87	0.85	7
Second	1 (16)	91.17	0.8	1	82.35	1	0.68	3
	2 (560)	82.35	1	0.68	88.24	0.87	0.9	9
	3 (5824)	70.59	0.33	1	70.59	0.33	1	7
	4 (9984)	64.71	0.2	1	73.53	0.4	1	7

TABLE IV
THE CLASSIFICATION RESULTS OF NORMAL-ABNORMAL CASES BY USING THE ROIS OBTAINED FROM DDSM DATABASE

Packet	Scale (number of coefficients)	SVM			k-NN			
		Accuracy (%)	Specificity	Sensitivity	Accuracy (%)	Specificity	Sensitivity	k value
First	1 (16)	98.53	0.97	1	67.65	1	0.35	3
	2 (560)	83.82	0.74	0.94	66.18	1	0.32	3
	3 (5824)	72.06	0.71	0.74	64.71	1	0.29	3
	4 (9984)	83.82	1	0.68	67.65	1	0.35	3
Second	1 (16)	94.12	0.88	1	45.59	0.71	0.21	3
	2 (560)	80.88	0.68	0.94	61.77	1	0.24	3
	3 (5824)	72.06	0.68	0.77	63.24	1	0.27	3
	4 (9984)	83.82	1	0.68	67.65	1	0.35	3

The processes applied above are performed in the same manner to the other dataset obtained from DDSM database. Table IV illustrates the classification results of the normal-abnormal separation using the ROIs obtained from DDSM database. The maximum accuracy rates for the first packets of the scales are 98.53% for the SVM classifier with scale 1 and 67.65% for the k-NN classifier with scale 1 and 4. For the second packets, the maximum accuracy rates are 94.12% for the SVM classifier with scale 1 and 67.65% for the k-NN classifier with scale 4. The results for benign-malignant classification by using the ROIs obtained from DDSM database are shown in Table V. The maximum accuracy rates for the first packets of the scales are 85.3% for the SVM classifier with scale 1 and 2 and 67.65% for the k-NN classifier with all scales. For the second packets, those results are 91.18% for the SVM classifier with scale 1 and 88.24% for the k-NN classifier with scale 2.

VI. RESULT AND DISCUSSION

Considering the accuracy rates, the number of coefficients and sensitivity rates, scale 1 stands out among the others. When scale 1 solely taken into account, it is observed that the

second packet of it outperforms the others. The results of the classification corresponding to the packets which provide the best performance are shown in Fig. 3. The values in the figure belong to SVM classifier. Regarding the maximum accuracy results, the comparison of the results of the other studies that use wave atom transform is represented in Table VI. It can be noticed that these studies use ROIs in different sizes and numbers and they use only one database and one classifier. In this study, two databases and two classifiers are employed. The previous studies [22]-[24] use all coefficients of wave atom transform or all coefficients of the scales (combining the packets). Additionally, to increase the classification performance, these studies are employed an additional method. In this work, good classification results are obtained using much fewer coefficients and without using any other additional methods. Furthermore, while this study and only one another study [24] use all abnormalities, the others in the table classify the micro-calcifications.

TABLE V
THE CLASSIFICATION RESULTS OF BENIGN-MALIGNANT CASES BY USING THE ROIS OBTAINED FROM DDSM DATABASE

Packet	Scale (number of coefficients)	SVM			k-NN			
		Accuracy (%)	Specificity	Sensitivity	Accuracy (%)	Specificity	Sensitivity	k value
First	1 (16)	85.29	0.67	1	67.65	0.27	1	3
	2 (560)	85.28	0.67	1	67.65	0.27	1	3
	3 (5824)	67.65	0.27	1	67.65	0.27	1	3
	4 (9984)	58.82	1	0.26	67.65	0.27	1	3
Second	1 (16)	97.06	1	0.95	55.88	0	1	3
	2 (560)	85.29	0.67	1	67.65	0.27	1	3
	3 (5824)	67.65	0.27	1	67.65	0.27	1	3
	4 (9984)	58.82	1	0.26	67.65	0.27	1	3

TABLE VI
COMPARISON WITH THE RESULTS OF OTHER STUDIES

	ROIs	**Features**	**Accuracy**	**Classifier**
Rajesh et al. [22]	MIAS (207 ROI, 256x256 pixel, consists of normal and MC)	Energy of scale 1's coefficients	100% (N-A) 100% (B-M)	SVM
Elangeeran et al. [23]	DDSM (400 ROI, 512x512 pixel, consists of MC)	PCA of all scale's coefficients	96.19% (B-M)	CC_ELM
Gedik et al. [24]	MIAS (200 ROI, 128x128 pixel, consists of normal and All)	PCA of scale 2's coefficients All coefficients of scale 1	100% (N-A) 100% (B-M)	SVM
Present study	MIAS & DDSM (228 images, 128x128 pixel, consists of normal and All)	Coefficients of the second packet of scale 1 Coefficients of the second packet of scale 1	100% (N-A) 97.06% (B-M)	SVM SVM

N-A - Normal-Abnormal classification
B-M - Benign-Malignant classification
MC - Micro-calcification
All - All abnormalities

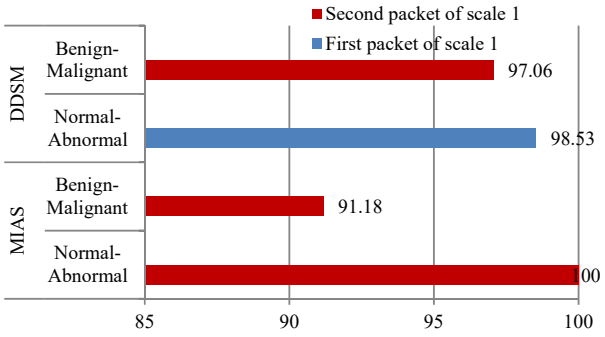

Fig. 3 The accuracy results for the packets which provide the best classification performance

VII. CONCLUSION

Considering a CAD system, feature extraction is a key step to achieve a more successful and faster system. An effective feature set can be determined with two distinguishing characteristics; having as many distinctive characteristics as possible, and having as small size as possible. This study investigates wave atom sub-bands to find out the most effective one or ones. Experimental results show that the coefficients belonging to the second packet of scale 1 have the best performance for both normal-abnormal and benign-malignant classification according to accuracy rates, the number of coefficients and sensitivity rates.

REFERENCES

[1] Y. Li, H. Chen, L. Cao, J. Ma, "A survey of computer-aided detection of breast cancer with mammography," *J Health Med Informat*, vol. 7, no. 4, pp. 238, 2016.
[2] Cheng H.D., Shan J., Ju W., Guo Y., Zhang L. "Automated breast cancer detection and classification using ultrasound images: a survey", *Pattern Recognit*., vol. 43, pp. 299–317, 2010.
[3] A. Jotwani, J. Gralow, "Early detection of breast cancer," *Mol. Diagn. Ther*., vol. 13, no. 6, pp. 349–357, 2009.
[4] J.L. Jasmine, S. Baskaran, A. Govardhan, "An automated mass

classification system in digital mammograms using contourlet transform and support vector machine," *Int. J. Comput. Appl*., vol. 31, no. 9, pp. 54–61, 2011.
[5] J. Dinnes, S. Moss, J. Melia, R. Blanks, F. Song, J. Kleijnen, "Effectiveness and cost-effectiveness of double reading of mammograms in breast cancer screening: findings of a systematic review," *The Breast*, vol. 10, no. 6, pp. 455–463, 2001.
[6] G. Zhang, P. Yan, H. Zhao, X. Zhang, "A computer-aided diagnosis system in mammography using artificial neural networks," *In BioMedical Engineering and Informatics 2008. International Conference on IEE;* China, 2008.
[7] S.D. Tzikopoulos, M.E. Mavroforakis, H.V. Georgiou, "A fully automated scheme for mammographic segmentation and classification based on breast density and asymmetry," *Computer methods and programs in biomedicine*, vol. 102, n. 1, pp. 47-63, 2011.
[8] T.M. Deserno, M Soiron., J.E.E. de Oliveira, A. de Araujo, "Towards computer-aided diagnostics of screening mammography using content-based image retrieval," *Proceedings of the Conference on Graphics, Patterns and Images (SIBGRAPI)*, Alagoas – Brazil, 2011**.**
[9] Z. Wang, G. Yu, Y. Kang, Y. Zhao, Q. Qu, "Breast tumor detection in digital mammography based on extreme learning machine," *Neurocomputing*, vol. 128, pp. 175-184, 2014.
[10] D. Moura, M. Guevara López, "An evaluation of image descriptors combined with clinical data for breast cancer diagnosis," *Int. J. Comp. Ass. Rad. Surg*., vol. 8, no. 4, pp. 561–574, 2013.
[11] S. Liu, C.F. Babbs, E.J. Delp, "Multiresolution detection of speculated lesions in digital mammograms," *Image Processing, IEEE Transactions on*, vol. 10, no. 6, pp. 874-884, 2001.
[12] C.B.R. Ferreira, D.L. Borges, "Analysis of mammogram classification using a wavelet transform decomposition," *Pattern Recognition Letters*, vol. 24, no. 7, pp. 973–982, 2003.
[13] S. Ergin, O. Kilinc, "A new feature extraction framework based on wavelets for breast cancer diagnosis," *Computers in Biology and Medicine*, vol. 51, pp. 171–182, 2014.
[14] F. Moayedi, Z. Azimifar, R. Boostani, S. Katebi, "Contourlet-based mammography mass classification using the SVM family," *Computers in Biology and Medicine*, vol. 40, no. 4, pp. 373-383, 2010.
[15] J.S. Leena Jasmine, S. Baskaran, A. Govardhan, "An automated mass classification system in digital mammograms using contourlet transform and support vector machine," *International Journal of Computer Applications*, vol. 31, no. 9, pp. 0975–8887, 2011.
[16] F. Pak, H.R Kanan., A. Alikhassi, "Breast cancer detection and classification in digital mammography based on non-subsampled contourlet transform (NSCT) and super-resolution," *Computer Methods and Programs in Biomedicine*, vol. 122, no. 2, pp. 89–107, 2015.
[17] M.M. Eltoukhy, I. Faye, B.B. Samir, "Breast cancer diagnosis in digital mammogram using multi-scale curvelet transform," *Computerized Medical Imaging and Graphics*, vol. 34, pp. 269–276, 2010.
[18] S.V. Francis, M. Sasikala, S. Saranya, "Detection of breast abnormality from thermograms using curvelet transform based feature extraction," *Journal of Medical Systems*, vol. 38, pp. 1-23, 2014.
[19] J. Ma, "Characterization of textural surfaces using wave atoms," *Applied Physics Letters*, vol. 90, pp. 264101, 2007.
[20] Z. Haddad, A. Beghdadi, A. Serir, A. Mokraou, "Image quality assessment based on wave atoms transform," *Proceedings of 2010 IEEE 17th International Conference on Image Processing;* Hong Kong, 2010.
[21] J. Rajeesh, R.S. Moni, S.S. Kumar, "Performance analysis of wave atom transform in texture classification," *Signal, Image and Video Processing*, vol. 8, pp. 923–930, 2014.
[22] A. Rajesh, M. Ellappan, "Classification of micro-calcification based on wave atom transform," *Journal of Computer Science*, vol. 10, no. 8, pp. 1543-1547, 2014.
[23] M. Elangeeran, S. Ramasamy, K. Arumugam, "A novel method for benign and malignant characterization of mammographic microcalcifications employing wave atom features and circular complex valued–extreme learning machine," *IEEE Ninth International Conference on Intelligent Sensors, Sensor Networks and Information Processing (ISSNIP) Symposium on Cognitive Computing in Information Processing;* Singapore, 2014.
[24] N. Gedik, A. Atasoy, "Performance evaluation of the wave atom algorithm to classify mammographic images," *Turk. J. Elec. Eng. & Comp. Sci.*, vol. 22, pp. 957–969, 2014.
[25] L. Demanet, L. Ying, "Wave atoms and sparsity of oscillatory patterns," *Appl. Comput. Harmon Anal*., vol. 23, pp. 368–387, 2007.
[26] MIAS database, http://peipa.essex.ac.uk/info/mias.html. (10.09.2017).
[27] DDSM database, http://marathon.csee.usf.edu/Mammography/Database.html. (10.09.2017).